

Mitochondrial morphology transition is an early indicator of subsequent cell death in *Arabidopsis*

Iain Scott and David C. Logan

Sir Harold Mitchell Building, School of Biology, University of St Andrews, St Andrews KY16 9TH, UK

Summary

Author for correspondence:

David C. Logan

Tel: +44 (0) 1334 463367

Fax: +44 (0) 1334 463366

Email: david.logan@st-andrews.ac.uk

Received: 3 August 2007

Accepted: 12 August 2007

- Mitochondrial morphology and dynamics were investigated during the onset of cell death in *Arabidopsis thaliana*. Cell death was induced by either chemical (reactive oxygen species (ROS)) or physical (heat) shock.
- Changes in mitochondrial morphology in leaf tissue, or isolated protoplasts, each expressing mitochondrial-targeted green fluorescent protein (GFP), were observed by epifluorescence microscopy, and quantified.
- Chemical induction of ROS production, or a mild heat shock, caused a rapid and consistent change in mitochondrial morphology (termed the mitochondrial morphology transition) that preceded cell death. Treatment of protoplasts with a cell-permeable superoxide dismutase analogue, TEMPOL, blocked this morphology change. Incubation of protoplasts in micromolar concentrations of the calcium channel-blocker lanthanum chloride, or the permeability transition pore inhibitor cyclosporin A, prevented both the mitochondrial morphology transition and subsequent cell death.
- It is concluded that the observed mitochondrial morphology transition is an early and specific indicator of cell death and is a necessary component of the cell death process.

Key words: *Arabidopsis*, cell death, mitochondria, mitochondrial dynamics, mitochondrial permeability transition, morphology.

New Phytologist (2008) **177**: 90–101

© The Authors (2007). Journal compilation © *New Phytologist* (2007)

doi: 10.1111/j.1469-8137.2007.02255.x

Introduction

Although chiefly associated with energy transduction, mitochondria are involved in a range of biosynthetic reactions that are essential to sustain eukaryotic life (Tzagoloff, 1982; Scheffler, 1999; Nunes-Nesi & Fernie, 2007). Equally, mitochondria play an important role in the ending of life, notably through the process of programmed cell death (PCD; for reviews see Lam *et al.*, 2001; Okamoto & Shaw, 2005; Youle & Karbowski, 2005).

In animals, mitochondria are intimately linked with PCD. The application of pro-death stimuli to mammalian cells leads to loss of mitochondrial transmembrane potential, changes in mitochondrial morphology, and the release of cytochrome *c*, which initiates several downstream processes (such as the

activation of cell-degrading caspase proteases) that culminate in cell death (Liu *et al.*, 1996; Skulachev, 1996; Zou *et al.*, 1997). In plants, the initiation of PCD also leads to the loss of mitochondrial transmembrane potential (Yao *et al.*, 2004), and the release of cytochrome *c* from mitochondria into the cytoplasm, which results in cell death (Balk *et al.*, 1999; Balk & Leaver, 2001; Yao *et al.*, 2004; Vacca *et al.*, 2006). Previous studies have shown that reactive oxygen species (ROS) may have an important function in plant cell death. In tobacco (*Nicotiana tabacum*), heat-induced cell death leads to sharp increases in intracellular ROS, and these changes are closely correlated with a loss of mitochondrial function and PCD (Vacca *et al.*, 2004). While preliminary observations suggested that ROS have the capacity to alter mitochondrial morphology in plants (Yoshinaga *et al.*, 2005), any causal link remained to be established.

Therefore, while we know much about the biochemical properties of ROS and mitochondria during PCD in plants, there has been little detailed research on the role of mitochondrial morphology during the cell death process. Using a range of external stimuli to induce cell death in both intact leaves and protoplasts of *Arabidopsis*, we have investigated the relationship between mitochondrial morphology and death. Here we report that a mild heat shock, or treatment with strong oxidants, induced a very rapid transition in mitochondrial morphology, which preceded subsequent cell death. Disruption of cellular calcium flux, or inhibition of the mitochondrial permeability transition pore, arrested the mitochondrial morphology transition and cell death, indicating a role for both factors in these processes.

Materials and Methods

Plant material and growth conditions

Seeds of lines 43C5 (mito-GFP wild type; Logan & Leaver, 2000) and the *network* (*nmt*) mitochondrial mutant (Logan *et al.*, 2003) were surface-sterilized, spread on Murashige & Skoog medium (MS) agar plates and allowed to stratify for 3 d at 4°C. Petri dishes containing stratified seeds were placed in a growth chamber (140 $\mu\text{mol m}^{-2}$ photosynthetic photon flux density (PPFD) on a 16-h light: 8-h dark cycle at 22–25°C) for 14–18 d.

Protoplast isolation

Under aseptic conditions, healthy leaves from 15 to 20 14–18-d-old plants were removed, sliced with a razor blade into four to six pieces in a Petri dish and washed in 15 ml of 0.5 M mannitol for 1 h. The wash solution was replaced with 15 ml of protoplast enzyme solution (0.4 M mannitol, 0.33% (weight/volume (w/v)) cellulase 'onozuka' R-10 (Yakult Honsha Co. Ltd., Tokyo, Japan), 0.17% (w/v) pectinase (Sigma, Poole, UK), 3 mM MES, and 7 mM CaCl_2 , pH 5.7). The Petri dish was sealed with Nescofilm (Bando Chemical Ind. Ltd., Kobe, Japan) and placed on an orbital shaker (~40–50 r.p.m.) overnight in the dark at room temperature. Protoplasts were isolated by filtration through 100- and 40- μm nylon mesh sieves and collected by centrifugation at 50 g for 10 min. Protoplasts were washed three times in 0.5 M mannitol and the concentration adjusted to between 10^{-5} and 10^{-6} protoplasts ml^{-1} with additional 0.5 M mannitol.

Application of chemical and heat treatments

Methyl viologen (Sigma), *s*-triazine (Sigma), and hydrogen peroxide (VWR, Lutterworth, UK) were adjusted to the appropriate concentration using sterile ultrapure H_2O (s. H_2O ; for use on leaves) or 0.5 M mannitol (protoplasts). Methyl viologen is a bipyridyl herbicide that donates electrons to oxygen within the cell, producing superoxide (O_2^- ; Halliwell & Gutteridge, 1985). Methyl viologen accepts electrons from chloroplast

photosystem I, producing O_2^- in the light (Tsang *et al.*, 1991). It also uncouples oxidative phosphorylation and reacts with endoplasmic reticulum NADPH-reductase, ensuring that O_2^- is also produced in the dark (Halliwell & Gutteridge, 1985; Palmeira *et al.*, 1995). In contrast, *s*-triazine binds specifically to the D1 protein of chloroplast photosystem II and blocks only the chloroplast electron transport chain (Ikeda *et al.*, 2003). Therefore, while methyl viologen produces O_2^- in light and dark conditions, *s*-triazine only produces O_2^- in the light. To treat leaves, 14–18-d-old seedlings were transferred to fresh MS agar plates and arranged in a well-spaced pattern. Three microlitres of either chemical, or s. H_2O (control), was placed onto the upper surface of each expanded leaf using a pipette. Seedlings were incubated in the growth room for 4 or 24 h under illumination or total darkness. To treat protoplasts, ROS-inducing chemicals in 0.5 M mannitol were added to 100 μl of protoplast suspension in a microfuge tube and incubated for the required period of time on a gentle rotary mixer at room temperature (18–25°C) in the dark (< 0.1 $\mu\text{mol m}^{-2}$ PPFD). For heat treatments, 100 μl of protoplast suspension in a microfuge tube was placed in a preheated circulating water bath at 45°C for 10 min; subsequent incubation was at room temperature with gentle mixing as already described. To determine the effect of calcium flux, LaCl_3 (Sigma) was added to 50 μM (from stock solution in 0.5 M mannitol) and protoplasts were incubated for 10 min before heat treatment. Serial dilution experiments were performed to determine a noncytotoxic LaCl_3 concentration (data not shown). To inhibit the formation of the permeability transition pore, protoplasts were incubated in 0.5 M mannitol containing 5 μM cyclosporin A (CsA; Sigma) for 20 min before heat treatment. To establish if chemical inhibition of ROS accumulation could prevent changes in mitochondrial morphology, protoplasts were incubated in 0.5 M mannitol containing 0.5–2 mM TEMPOL (a synthetic, membrane-permeable superoxide dismutase analogue; Laight *et al.*, 1997; Latifi *et al.*, 2005) for 30 min before the addition of methyl viologen or heat treatment.

Mitochondrial morphology and measurement of cell death

To determine mitochondrial morphology, protoplasts were examined and quantified by epifluorescence microscopy. Protoplasts were deemed to have an abnormal mitochondrial population if more than half of the individual mitochondria had plan areas greater than twice that of mitochondria in untreated and control treated protoplasts. In addition to changes in size, abnormal mitochondria displayed changes in shape (from spherical or cigar-shaped to irregular teardrop or pear-shaped forms) and were often characterized by the appearance of green fluorescent protein (GFP) voids (areas where GFP fluorescence was greatly reduced or absent; see Supplementary Material Fig. S1). Approximately 100 protoplasts

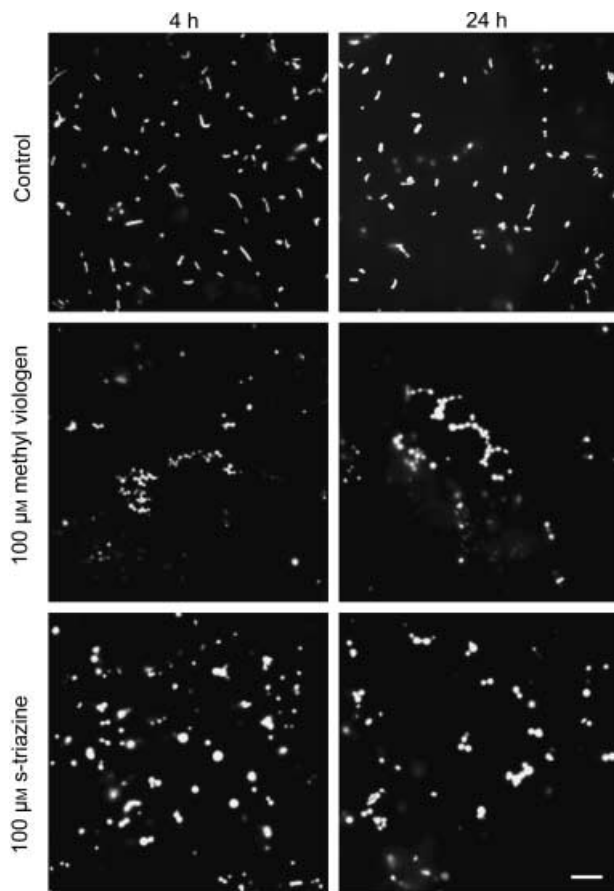


Fig. 1 Epifluorescence micrographs of mitochondrial morphology in *Arabidopsis* leaf tissue after treatment with reactive oxygen species (ROS)-inducing chemicals. Three microlitres of either 100 μM methyl viologen or 100 μM *s*-triazine was placed on the adaxial surface of one of the first true leaves of 14–18-d-old mito-GFP *Arabidopsis* seedlings (line 43C5) grown in a growth room (140 $\mu\text{mol m}^{-2} \text{s}^{-1}$ photosynthetic photon flux density (PPFD); 22–25°C) on agar plates. After treatment, plates were placed in the growth room for either 4 or 24 h constant light. Mitochondrial morphology was examined by epifluorescence microscopy. The control consisted of the application of 3 μl of sterile ultrapure H_2O ($\text{s}\text{-H}_2\text{O}$) for 4 or 24 h. Leaves of at least five plants were examined per treatment, and the experiment was performed three times. Micrographs are representative of the images obtained. Bar, 5 μm .

were analysed for each time-point and treatment, and the whole experiment was repeated twice using a different, freshly isolated protoplast preparation. Data are presented as means of three independent experiments \pm SE.

To determine cell viability, protoplasts were incubated for 5 min at room temperature in 0.002% (w/v) fluorescein diacetate (FDA; Sigma) in 0.5 M mannitol. Any intact protoplast that did not show FDA fluorescence was deemed to be dead. Approximately 200 protoplasts were measured for each treatment and time-point, and the whole experiment was repeated and the data were analysed as for morphology measurements.

Microscopy

For visualization of GFP, GFP and chlorophyll autofluorescence together, or FDA we used a Zeiss Axioskop 2 Plus epifluorescence microscope (Carl Zeiss Ltd, Welwyn Garden City, UK), fitted with a band-pass filter cube for GFP (filter set 13; excitation 470/20 nm; dichroic mirror 495 nm; emission 505–530 nm) and a long-pass filter cube (filter set 9; excitation 450–490 nm; dichroic mirror 510 nm; emission long pass (LP) 515 nm), and a $\times 20$ water and a $\times 100$ oil-immersion objective (Plan-Apochromat, numerical aperture = 1.4). For the capture of merged images of GFP fluorescence and chlorophyll autofluorescence we used an Olympus BX-40 epifluorescent microscope (Olympus Optical Co. (UK) Ltd, Southall, UK) fitted with cubes for GFP (Olympus U-M41001; excitation 480/40 nm; dichroic mirror 505 nm; emission 535/50 nm) and for chlorophyll autofluorescence (Olympus U-M41004; excitation 560/55 nm; dichroic mirror 595 nm; emission 645/75 nm) and a $\times 100$ oil-immersion objective (Universal Plan Fluorite; numerical aperture = 1.3; Olympus Optical Co. (UK) Ltd). Micrographs were captured using a monochrome digital camera (F-View; Soft Imaging System GmbH, Munster, Germany) linked to a computer, and images were stored and processed using the ANALYSIS image analysis software package (Soft Imaging System GmbH). The images in Supplementary Material Fig. S2 were false-coloured for GFP (green) and chloroplast autofluorescence (red) using Confocal Assistant (Bio-Rad, Hemel Hempsted, UK).

Results

Mitochondrial morphology in *Arabidopsis* leaves treated with ROS-inducing chemicals

After 4 h, mitochondria in leaves treated with 100 μM methyl viologen showed an aggregated distribution, with tens of mitochondria arranged into tight clusters (Fig. 1). Treatment with 100 μM *s*-triazine caused an increase in the plan areas of individual mitochondria relative to the controls (Fig. 1). After 24 h, the mitochondria in methyl viologen-treated leaves no longer formed extensive clumps. Instead they, like mitochondria in *s*-triazine-treated leaves, showed an increase in plan area relative to the control (Fig. 1).

The chondriome in the *network* (*nmt*) mitochondrial mutant (Logan *et al.*, 2003) exhibits a reticular phenotype, similar to that observed in animal cells. While the addition of $\text{s}\text{-H}_2\text{O}$ to illuminated leaves had no effect on mitochondrial morphology and structure in *nmt* mutants, treatment of leaves in the light with methyl viologen or *s*-triazine led to a disruption of the reticular chondriome and a concomitant increase in the number of physically discrete organelles (Fig. 2). Additionally, treatment with ROS-inducing chemicals led to the formation of mitochondria with an annular appearance (Fig. 2).

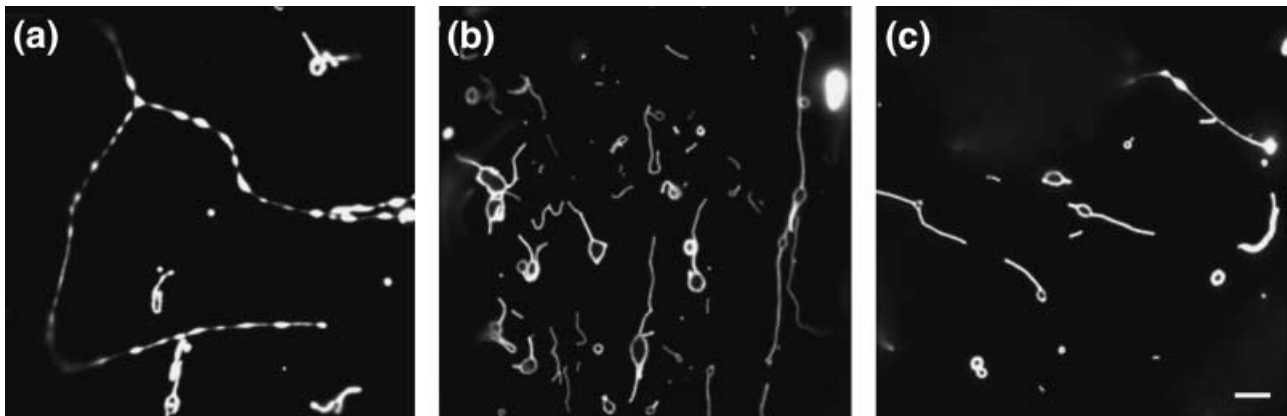


Fig. 2 Epifluorescence micrographs of mitochondrial morphology in *network* (*nmt*) *Arabidopsis* leaf tissue after treatment with reactive oxygen species (ROS)-inducing chemicals. Three microlitres of either (b) 100 μM methyl viologen or (c) 100 μM *s*-triazine was placed on the adaxial surface of one of the first true leaves of 14–18-d-old *Arabidopsis* seedlings (line *nmt*) grown in a growth room (140 $\mu\text{mol m}^{-2} \text{s}^{-1}$ photosynthetic photon flux density (PPFD); 22–25°C) on agar plates. After treatment, plates were placed in the growth room for 4 h. Mitochondrial morphology was examined by epifluorescence microscopy. The control (a) consisted of the application of 3 μl of sterile ultrapure H_2O (*s.H}_2\text{O}*) for 4 h. Leaves of at least five plants were examined per treatment, and the experiment was performed three times. Micrographs are representative of the images obtained. Bar, 5 μm .

Relationship between mitochondrial morphology and ROS

To establish if changes in mitochondrial morphology and distribution were ROS-specific, the effects of methyl viologen and *s*-triazine (two superoxide-producing chemicals with different modes of action; see Materials and Methods) were tested under light and dark conditions. In control plants treated with *s.H}_2\text{O}*, mitochondria retained a normal morphology when incubated under both light and dark conditions over 24 h. Mitochondria in both light- and dark-treated leaves were typically motile and had a cigar-shaped morphology (Fig. 3). Leaves treated with methyl viologen (which produces O_2^- in light and dark) contained mitochondria with an abnormal morphology after 24 h under both light and dark conditions, with the mitochondrial plan area much greater than in the control (Fig. 3). While leaves treated with *s*-triazine (produces O_2^- only under illumination) showed an abnormal mitochondrial morphology when illuminated, mitochondria in leaves placed in the dark showed no gross morphological change (Fig. 3).

Mitochondrial morphology and cell death in *Arabidopsis* protoplasts treated with ROS-inducing chemicals

To quantify the effect of ROS on mitochondrial morphology and cell viability, *Arabidopsis* mesophyll protoplasts expressing mito-GFP (line 43C5) were incubated with ROS-inducing chemicals. After 4 h of treatment with 50 μM methyl viologen, 50 μM *s*-triazine or 5 mM hydrogen peroxide, there was an increase in mitochondrial plan area, with protoplasts incubated in methyl viologen often containing tubular and annular

mitochondria (Fig. 4a). At 4 h, $24.2 \pm 0.9\%$ (mean \pm SE) of protoplasts in the control treatment (0.5 M mannitol only) contained abnormal mitochondria, compared to means of $61.3 \pm 3.1\%$, $56.4 \pm 3.2\%$ and $58.3 \pm 3.5\%$ for 50 μM methyl viologen, 50 μM *s*-triazine and 5 mM hydrogen peroxide, respectively (Fig. 4b). By 48 h, 66–73% of cells treated with methyl viologen, *s*-triazine or hydrogen peroxide displayed an abnormal mitochondrial morphology, compared with $29.1 \pm 3.2\%$ of protoplasts in the control (Fig. 4b).

The addition of the ROS scavenger TEMPOL to methyl viologen-treated protoplasts led to a decrease in the number of cells with abnormal mitochondria. While $73.4 \pm 1.9\%$ of protoplasts treated with methyl viologen displayed an abnormal mitochondrial morphology after 4 h of treatment, this was reduced to only $53.8 \pm 2.6\%$ by preincubation with 0.5 mM TEMPOL before methyl viologen treatment (Fig. 4c). Increasing concentrations of this scavenger ameliorated the effect of methyl viologen, such that only $27.2 \pm 2.5\%$ of protoplasts preincubated in 2 mM TEMPOL showed an abnormal mitochondrial phenotype after 4 h of treatment with methyl viologen (Fig. 4c), a result that was not significantly different from that for the control ($24.2 \pm 0.9\%$; Student's *t*-test: $t = 1.13$, $P = 0.16$, d.f. = 4).

Control-treated protoplasts remained viable throughout the experiment, with only $9.6 \pm 2.5\%$ of protoplasts dying after 48 h (Fig. 4d). Up to 24 h after the initiation of treatment, cell death in the three ROS treatments remained largely similar to that in controls, with the methyl viologen and *s*-triazine treatments displaying $11.8 \pm 4.2\%$ and $8.7 \pm 0.6\%$ cell death, respectively. Only the hydrogen peroxide treatment showed a significant increase in cell death at 24 h, with a mean of $15.6 \pm 3.6\%$ (Student's *t*-test: $t = 2.19$, $P < 0.05$, d.f. = 4; Fig. 4d). Changes in cell viability in the ROS treatments were

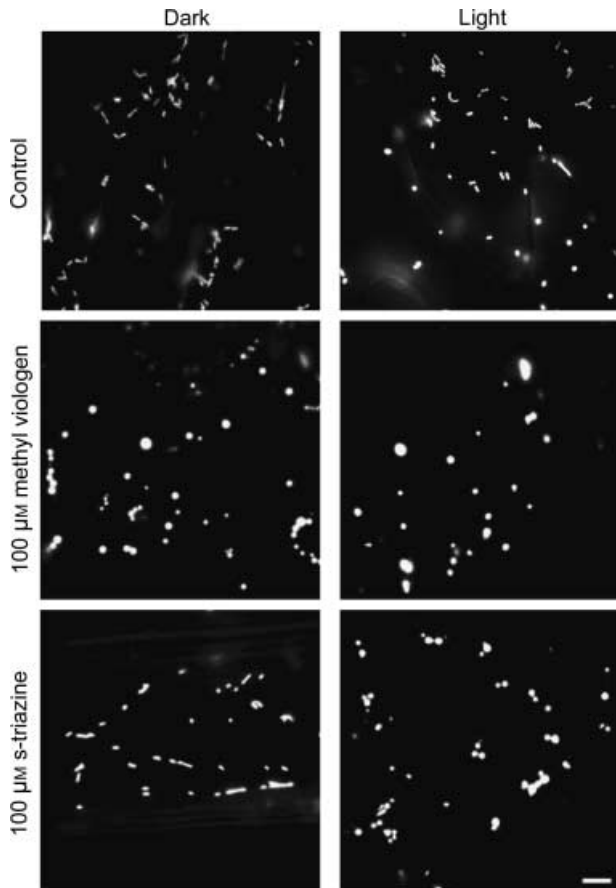


Fig. 3 Epifluorescence micrographs of mitochondrial morphology in *Arabidopsis* leaf tissue after treatment with reactive oxygen species (ROS)-inducing chemicals for 24 h under light and dark conditions. Three microlitres of either 100 μM methyl viologen or 100 μM *s*-triazine was placed on the adaxial surface of one of the first true leaves of 14–18-d-old *Arabidopsis* seedlings (line 43C5) grown on agar plates in a growth room (140 $\mu\text{mol m}^{-2} \text{s}^{-1}$ photosynthetic photon flux density (PPFD); 22–25°C). After treatment, plates were placed in the growth room for 24 h under full illumination, or in total darkness (growth room, lights switched off). Mitochondrial morphology was examined by epifluorescence microscopy. The control consisted of the application of 3 μl of sterile ultrapure H_2O (*s.H*₂O) for 24 h. Leaves of at least five plants were examined per treatment, and the experiment was performed three times. Micrographs are representative of the images obtained. Bar, 5 μm .

clear at 48 h, with all three treatments causing 64–71% cell death; six to seven times greater than the control at $9.6 \pm 2.5\%$ (Fig. 4d). There were no changes observed in chloroplast gross morphology following ROS treatment of protoplasts (Supplementary Material Fig. S2).

Mitochondrial morphology and cell death in *Arabidopsis* protoplasts following heat treatment

Five minutes after the end of heat treatment (45°C for 10 min), $68.6 \pm 6.1\%$ of heat-treated protoplasts contained abnormal

mitochondria, rising to $72.6 \pm 1.5\%$ 24 h after the end of the heat treatment (Fig. 5a,b). Only $22.1 \pm 2.1\%$ of protoplasts in the control treatment (15 min at room temperature instead of 10 min heat treatment and 5 min at room temperature) had aberrant mitochondrial morphology, rising slightly to $25.6 \pm 1.2\%$ after 24 h (Fig. 5b). Incubating protoplasts in the most effective concentration of TEMPOL (2 mM) before heat treatment reduced the proportion of cells with abnormal mitochondria. Five minutes after heat treatment, $68.6 \pm 6.1\%$ of protoplasts displayed abnormal mitochondria, compared with $28.0 \pm 1.2\%$ of those preincubated with TEMPOL (Student's *t*-test: $t = 6.5$, $P < 0.01$, d.f. = 4; Fig. 5c). There was no significant difference between protoplasts maintained at room temperature (control, $22.1 \pm 2.1\%$) and those subjected to heat plus TEMPOL treatment (Student's *t*-test: $t = 2.43$, $P < 0.05$, d.f. = 4; Fig. 5c).

There was no significant difference in the incidence of cell death in heat-treated relative to unheated control protoplast samples for the first 4 h post-treatment; however, $16.6 \pm 1.5\%$ of protoplasts died within the first 8 h after heat treatment, compared with $10.6 \pm 0.8\%$ in the unheated control (Student's *t*-test: $t = 3.31$, $P < 0.05$, d.f. = 4; Fig. 5d). By 24 h, $64.8 \pm 6.4\%$ of heat-treated protoplasts were dead (FDA-negative), compared with only $11.4 \pm 0.1\%$ in the control (Student's *t*-test: $t = 8.32$, $P < 0.01$, d.f. = 4; Fig. 5d). To determine whether or not there is a correlation between cell death and mitochondrial morphology, the morphology of mitochondria in intact dead protoplasts was quantified 24 h after the 10-min heat treatment. $94.6 \pm 0.3\%$ of FDA-negative (dead) protoplasts contained abnormal mitochondria (Fig. 5e). A similar analysis could not be performed on living protoplasts because the relatively bright FDA fluorescence could not be separated from the relatively weak fluorescence of mito-GFP, precluding any examination of mitochondrial morphology. There were no changes observed in chloroplast gross morphology following the heat treatment of protoplasts (Supplementary Material Fig. S2).

The role of calcium in mitochondrial morphology and cell death

As a first step to investigating any role for calcium dynamics in mitochondrial morphology and cell viability, protoplasts were incubated in lanthanum chloride (LaCl_3) for 10 min before heat treatment. Incubation in LaCl_3 before heat treatment led to a large decrease in the number of protoplasts exhibiting an abnormal mitochondrial morphology: after 5 min $68.6 \pm 6.1\%$ showed a morphology transition in the heat minus LaCl_3 group, compared with $34.5 \pm 1.7\%$ in the heat plus LaCl_3 group (Student's *t*-test: $t = 5.35$, $P < 0.01$, d.f. = 4; Fig. 6a). Between 1 and 24 h, there was a small increase in the number of protoplasts exhibiting abnormal mitochondrial morphology ($68.3 \pm 3.0\%$ to $72.6 \pm 1.5\%$) in the heat minus LaCl_3 group, compared with a decrease

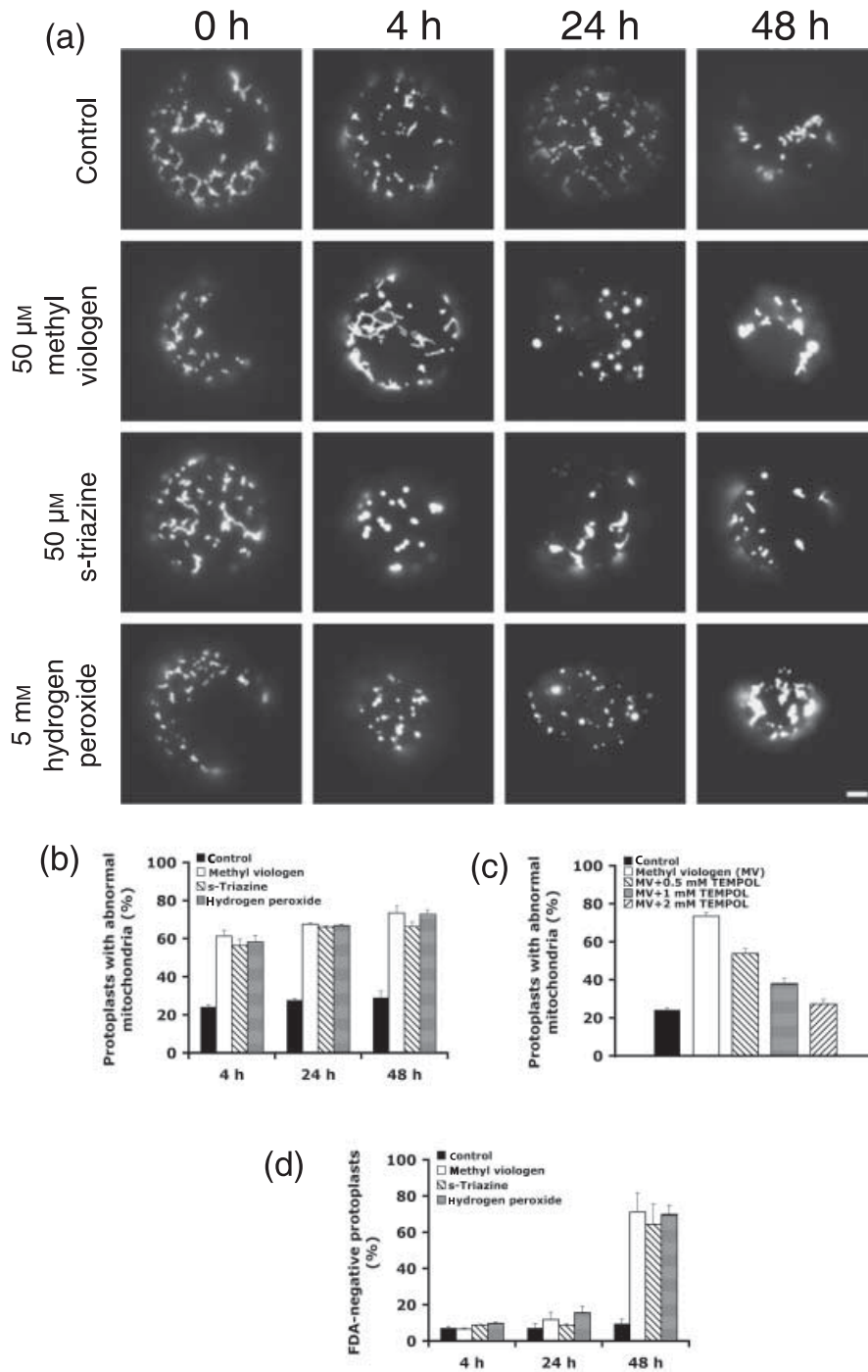


Fig. 4 Abnormal mitochondrial morphology and cell death in Arabidopsis mesophyll protoplasts after treatment with reactive oxygen species (ROS)-inducing chemicals. Arabidopsis mesophyll protoplasts were incubated in 0.5 M mannitol containing 50 μM methyl viologen, 50 μM s-triazine or 5 mM hydrogen peroxide with gentle mixing for 4, 24 or 48 h at room temperature ($< 0.1 \mu\text{mol m}^{-2} \text{s}^{-1}$ photosynthetic photon flux density (PPFD); 18–25°C). The control was 0.5 M mannitol only. (a) Epifluorescence micrographs of mitochondrial morphology in Arabidopsis mesophyll protoplasts before and after treatment. Bar, 5 μm . (b) Percentage of protoplasts with abnormal mitochondrial morphology. Data are presented as means \pm SE of three experiments, with *c.* 100 protoplasts per experiment. (c) Effect of the ROS scavenger TEMPOL on mitochondrial morphology. Protoplasts were incubated in 0.5–2 mM TEMPOL for 30 min before methyl viologen treatment; mitochondrial morphology was determined after 4 h as above. Data are presented as means \pm SE of three experiments, with *c.* 100 protoplasts per experiment. (d) Percentage of protoplasts negative for the vital stain fluorescein diacetate (FDA). Protoplasts were incubated for 5 min in 0.002% (weight/volume) FDA. Protoplasts were examined by epifluorescence microscopy and intact nonfluorescing cells were deemed dead. Data are presented as means \pm SE of three experiments, with *c.* 200 protoplasts per experiment.

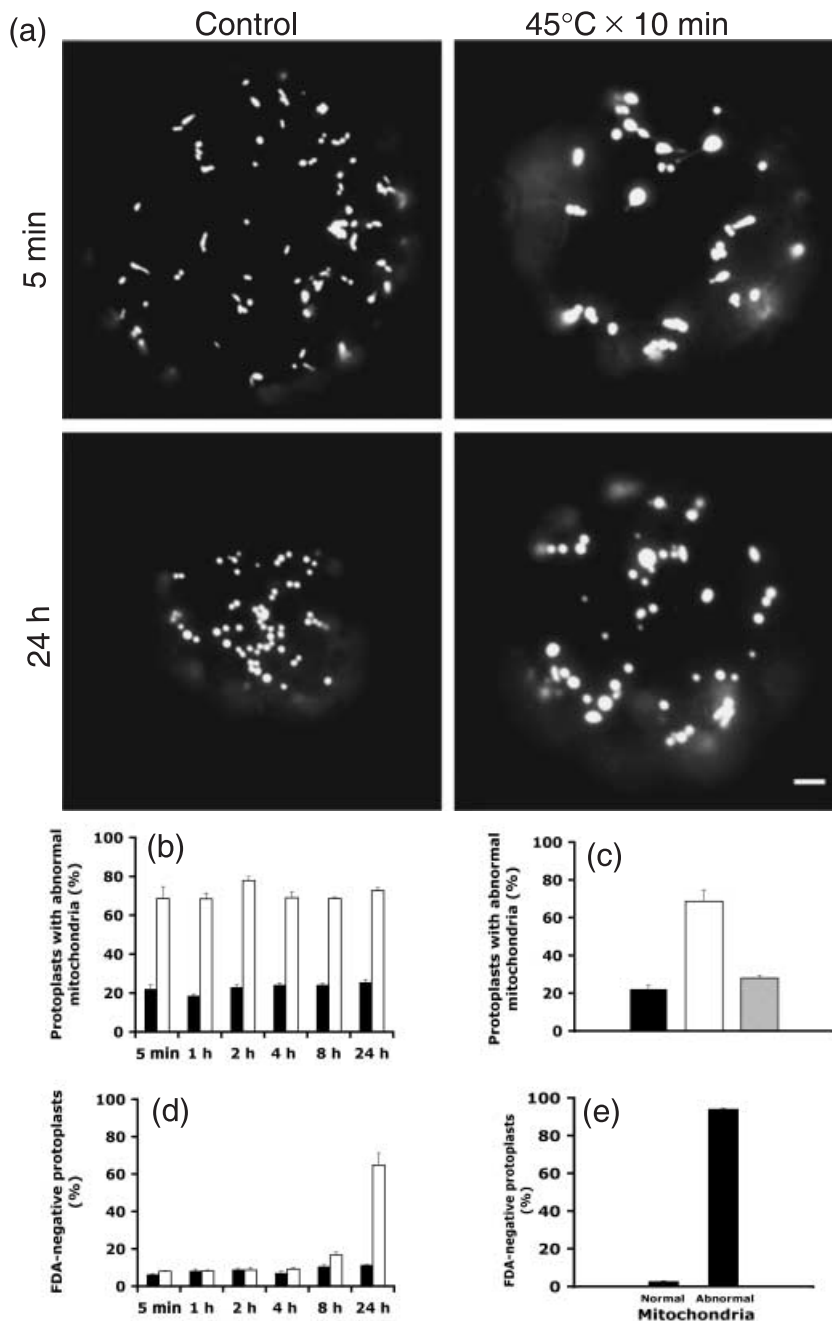


Fig. 5 Abnormal mitochondrial morphology and cell death in Arabidopsis mesophyll protoplasts after 45°C heat treatment (HT). Arabidopsis mesophyll protoplasts (line 43C5) were incubated in 0.5 M mannitol for 10 min at 45°C in a water bath, and then transferred to room temperature (with gentle mixing) for periods of 5 min to 24 h ($< 0.1 \mu\text{mol m}^{-2} \text{s}^{-1}$ photosynthetic photon flux density (PPFD); 18–25°C). Control protoplasts were maintained in 0.5 M mannitol at room temperature with gentle mixing. (a) Epifluorescence micrographs of mitochondrial morphology in Arabidopsis mesophyll protoplasts after 45°C heat treatment. Bar, 5 μm. (b) Percentage of protoplasts with abnormal mitochondrial morphology. Data are presented as means \pm SE of three experiments, with *c.* 100 protoplasts per experiment. Control, closed bars; HT, open bars. (c) Effect of the reactive oxygen species (ROS) scavenger TEMPOL on mitochondrial morphology. Protoplasts were incubated in 2 mM TEMPOL for 30 min before heat treatment and mitochondrial morphology was determined after 5 min as above. Data are presented as means \pm SE of three experiments, with *c.* 100 protoplasts per experiment. Control, closed bars; HT, open bars; HT + TEMPOL, grey bars. (d) Percentage of protoplasts negative for fluorescein diacetate (FDA) fluorescence. Protoplasts were incubated for 5 min in 0.002% (weight/volume (w/v)) FDA. Protoplasts were examined by epifluorescence microscopy and intact nonfluorescing cells were deemed dead. Data are presented as means \pm SE of three experiments, with *c.* 200 protoplasts per experiment. Control, closed bars; HT, open bars. (e) Relationship between cell death and abnormal mitochondrial morphology. Protoplasts were incubated in 0.5 M mannitol for 10 min at 45°C in a water bath, and then transferred to room temperature for 24 h. After this time, protoplasts were incubated in 0.002% (w/v) FDA for 5 min and examined by epifluorescence microscopy. The proportions of intact FDA-negative (dead) protoplasts with normal and abnormal mitochondrial morphology were determined. Data are presented as means \pm SE of three experiments, with 50 protoplasts analysed per experiment.

(37.5 \pm 2.9% to 25.2 \pm 2.6%) over the same period in the heat plus LaCl₃ group (Fig. 6a). Without heat treatment, the addition of LaCl₃ led to some minor, although statistically significant, changes in mitochondrial morphology. However, there was no obvious trend over the course of the experiment, with changes alternating between the plus and minus LaCl₃ controls at each time-point from 5 min to 24 h (Fig. 6a).

Cell viability was also affected by the addition of LaCl₃. In the controls (no heat), there was no significant difference in the percentage of FDA-negative (dead) cells after the addition of LaCl₃ over 24 h. Death in the minus heat/minus LaCl₃ group ranged from 6.3 to 11.3% over 24 h, while in the minus heat/plus LaCl₃ control, 5.3–13.5% of cells were FDA-negative in the same period (Fig. 6b). In heat-treated samples

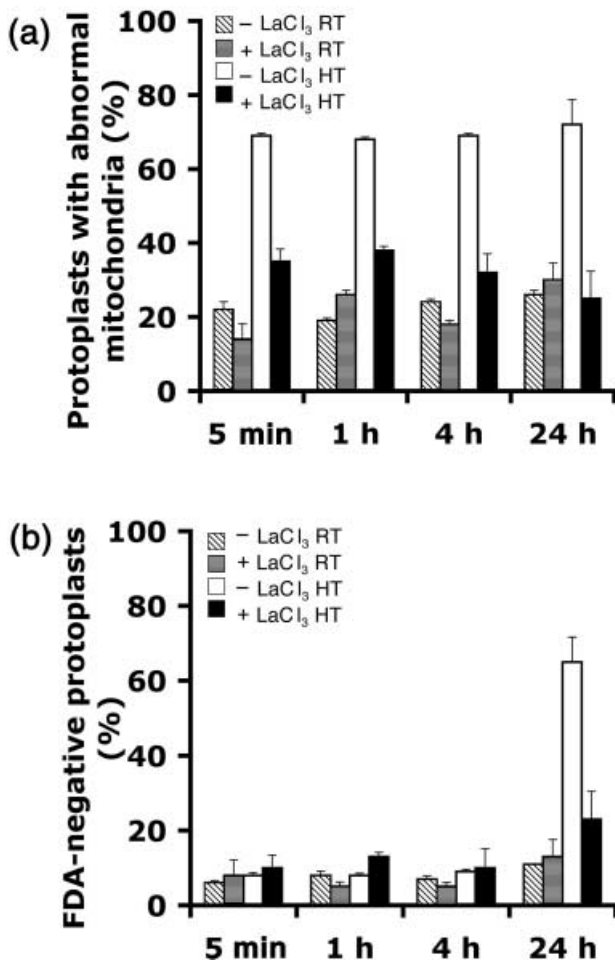


Fig. 6 Effect of lanthanum chloride on mitochondrial morphology and cell death in *Arabidopsis* mesophyll protoplasts. *Arabidopsis* mesophyll protoplasts (line 43C5) were incubated in 0.5 M mannitol \pm 50 μ M lanthanum chloride (LaCl₃) for 10 min before being placed in a 45°C water bath for 10 min. After this time, protoplasts were transferred to room temperature (RT) with gentle mixing for periods of 5 min to 24 h ($<$ 0.1 μ mol m⁻² s⁻¹ photosynthetic photon flux density (PPFD); 18–25°C). Control protoplasts were maintained in 0.5 M mannitol \pm 50 μ M lanthanum chloride at room temperature with gentle mixing. (a) Percentage of protoplasts with abnormal mitochondrial morphology. Data are presented as means \pm SE of three experiments, with *c.* 100 protoplasts per experiment. (b) Percentage of protoplasts negative for fluorescein diacetate (FDA) fluorescence. Protoplasts were incubated for 5 min in 0.002% (weight/volume) FDA. Protoplasts were examined by epifluorescence microscopy and intact nonfluorescing cells were deemed dead. Data are presented as means \pm SE of three experiments, with *c.* 200 protoplasts per experiment.

the addition of LaCl₃ before heating significantly reduced subsequent cell death: 64.8 \pm 6.4% of protoplasts died within 24 h in the absence of LaCl₃, compared with 31.7 \pm 0.7% when incubated with LaCl₃ (Student's *t*-test: *t* = 4.25, *P* < 0.01, d.f. = 4; Fig. 6b).

The function of the mitochondrial permeability transition pore in mitochondrial morphology and cell death

To explore whether the observed changes in mitochondrial morphology and cell death were related to the previously described mitochondrial permeability transition, protoplasts were incubated in the permeability transition pore inhibitor CsA for 20 min before heat treatment. Five minutes after heat treatment, 55.0 \pm 4.2% of protoplasts incubated in CsA displayed abnormal mitochondria, compared with 75.3 \pm 0.9% of cells in the minus CsA treatment (Student's *t*-test: *t* = 4.77, *P* < 0.01, d.f. = 4; Fig. 7a). This significant difference in mitochondrial morphology was maintained over the course of the experiment, such that by 24 h 81 \pm 3.2% of protoplasts in the minus CsA group had an abnormal mitochondrial morphology, compared with 55.3% \pm 3.4 of those with CsA (Student's *t*-test: *t* = 5.5, *P* < 0.01, d.f. = 4; Fig. 7b).

In addition to reducing the percentage of protoplasts containing abnormal mitochondria, incubation with CsA reduced cell death. While there was no significant difference in cell viability between the two groups at 5 min and 1 h (for example, 5.7 \pm 1.4% FDA-negative protoplasts in the minus CsA group, compared with 5.7 \pm 1.7% in the plus CsA group at 1 h; Fig. 7b), the effect of CsA became apparent at 24 h. At this time-point, 20.9 \pm 12.8% of protoplasts incubated with CsA before heat treatment were FDA-negative, compared with 59.4 \pm 6.3% of those in the minus CsA group (Student's *t*-test: *t* = 2.7, *P* < 0.05, d.f. = 4; Fig. 7b). Throughout the experiment there was no measurable difference in mitochondrial morphology, or cell viability, between plus and minus CsA-incubated protoplasts not subject to heat treatment (data not shown).

Discussion

Chemical or physical induction of cell death causes a rapid change in gross mitochondrial morphology, visible in optical sections as an increase in the plan area of individual mitochondria (Figs 1, 4a, 5a). This mitochondrial morphology transition is likely to be indicative of, and therefore synonymous with, the mitochondrial permeability transition (MPT). The MPT has been described in plants following the chemical treatment of mitochondria isolated from potato (*Solanum tuberosum*) and oat (*Avena sativa*; Arpagaus *et al.*, 2002; Curtis & Wolpert, 2002), and is characterized by several features, including the loss of transmembrane electrical potential ($\Delta\Psi_m$), and the proposed formation of the permeability transition pore (PTP; Zoratti & Szabo, 1995; Skulachev, 1996; Zoratti *et al.*, 2005; Vacca *et al.*, 2006). This pore (proposed to be composed of the voltage-dependant anion channel (VDAC), adenine nucleotide transporter (ANT) and cyclophilin D (for reviews, see Lee *et al.*, 2004; Tsujimoto *et al.*, 2006)) allows the movement of water and solutes into the mitochondrial matrix, causing

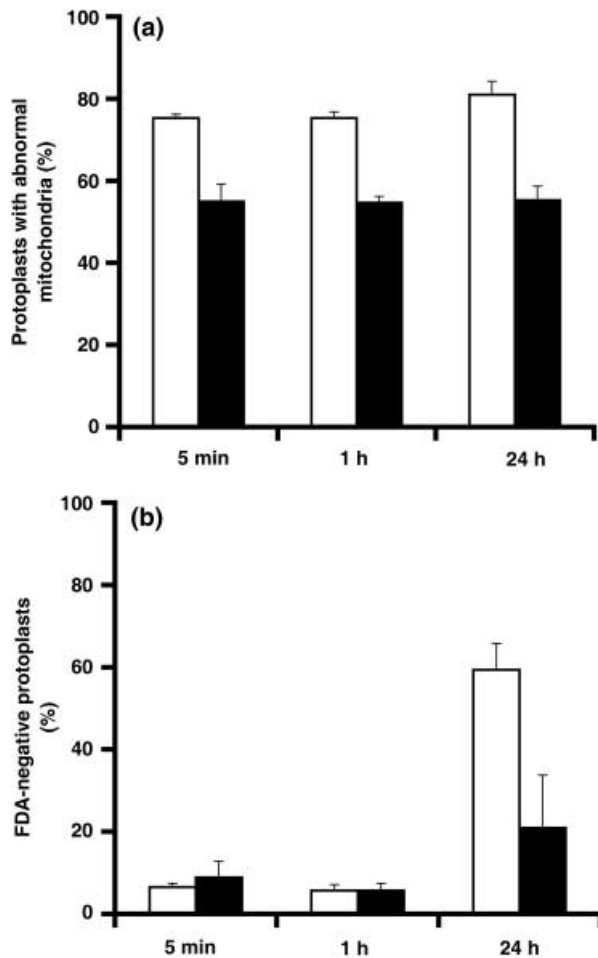


Fig. 7 Effect of cyclosporin A on mitochondrial morphology and cell death in *Arabidopsis* mesophyll protoplasts. *Arabidopsis* mesophyll protoplasts (line 43C5) were incubated in 0.5 M mannitol \pm 5 μ M cyclosporin A (CsA) for 20 min before being placed in a 45°C water bath for 10 min. After this time, protoplasts were transferred to room temperature with gentle mixing for periods of 5 min to 24 h ($<$ 0.1 μ mol m⁻² s⁻¹ photosynthetic photon flux density (PPFD); 18–25°C). (a) Percentage of protoplasts with abnormal mitochondrial morphology. Data are presented as means \pm SE of three experiments, with *c.* 100 protoplasts per experiment. (b) Percentage of protoplasts negative for fluorescein diacetate (FDA) fluorescence. Protoplasts were incubated for 5 min in 0.002% (weight/volume) FDA. Protoplasts were examined by epifluorescence microscopy and intact nonfluorescing cells were deemed dead. Data are presented as means \pm SE of three experiments, with *c.* 200 protoplasts per experiment. Open bars, minus CsA; closed bars, plus CsA.

the organelle to swell. The MPT can be inhibited by disrupting proposed members of the PTP with the addition of bonkreikic acid (a ligand of the ANT), or cyclosporin A (which binds to cyclophilin D; Tsujimoto *et al.*, 2006). We tested one of these chemicals, cyclosporin A, and found that it reduced the mitochondrial morphology transition seen after the induction of cell death (Fig. 7), indicating a link between this process and the MPT. Aquaporins have also recently been implicated

in the MPT (Lee & Thevenod, 2006). Swelling can cause the outer mitochondrial membrane to rupture, aiding the release of inner membrane space proteins such as cytochrome *c*.

Our results demonstrate that the mitochondrial morphology transition can be observed much earlier than similar changes in morphology previously reported *in vivo* (Yoshinaga *et al.*, 2005; Zottini *et al.*, 2006). Using protoplasts we observed changes in mitochondrial morphology on a time-scale similar to that reported from *in vitro* experiments using isolated plant mitochondria (Figs 4, 5) where, for example, the addition of calcium chloride induced swelling within 5 min (Arpagaus *et al.*, 2002; Curtis & Wolpert, 2002). Preliminary data on the effects of ROS-inducing chemicals on mitochondrial morphology in whole *Arabidopsis* leaves indicated changes occurring between 24 and 72 h (Yoshinaga *et al.*, 2005); our results clearly demonstrate that the morphology transition is evident in leaves within 4 h (Fig. 1). Crucially, the use of methyl viologen and *s*-triazine in light and dark conditions, which provides a control for ROS production (Fig. 3), and the use of the ROS scavenger TEMPOL (Fig. 4c), which limits *in vivo* ROS concentration (Laight *et al.*, 1997; Latifi *et al.*, 2005), allow us to be confident that the measured effects on mitochondrial morphology were caused by ROS *per se*, and did not arise through an off-target effect of the ROS-inducing chemical, or as an artefact of the experimental method.

Mitochondrial division is a crucial starting point for cell death in mammalian cells (Frank *et al.*, 2001; Frank *et al.*, 2003; Jagasia *et al.*, 2005; Yu *et al.*, 2005). We have described how, in common with animal PCD, changes in mitochondrial morphology feature very early during plant cell death. The commonality of the responses to cell death triggers, at the level of the mitochondrion, are typified by the fragmentation of the reticular chondriome in the *Arabidopsis network* mutant following treatment with ROS-inducing chemicals (Fig. 2), mimicking the division of the mammalian chondriome after the induction of PCD. However, as the chondriome of plant cells typically exists as a population of numerous physically discrete organelles (Stickens & Verbelen, 1996; Logan & Leaver, 2000; Logan, 2006), rather than as a reticulum, an initial mass fragmentation event would seem redundant; although clearly our results using *network* suggest that the components required to execute mass division are present. We could see no evidence in our study for the initial decrease in the size of mitochondria reported in a previous study (Yoshinaga *et al.*, 2005) in response to applied ROS. Further, although Yoshinaga *et al.* (2005) related the apparent decrease in mitochondrial size to the fragmentation of the chondriome that occurs during mammalian apoptosis, no evidence was presented to support this, nor any evidence demonstrating the concomitant increase in the number of individual organelles that would be expected (Scott *et al.*, 2006). However, as Yoshinaga *et al.* (2005) also presented no direct data on the effect of ROS on mitochondrial morphology, or cell death, we cannot be sure of the relevance of that earlier work to ours. A robust investigation

of cell death using Arabidopsis division-gene mutants (Logan *et al.*, 2004; Scott, 2006; Scott *et al.*, 2006) should determine whether or not mitochondrial division is required for cell death in plants.

The protoplast system employed here has two main advantages. Previous measurements of the MPT following chemical treatment relied on spectrophotometric data relating to mitochondrial swelling *in vitro*; increased light scattering, presumably caused by organelle swelling, being used as a proxy for MPT induction (Arpagaus *et al.*, 2002; Curtis & Wolpert, 2002). In contrast, the methods used in this study allow a direct measurement of mitochondrial behaviour *in vivo*, making this a simple and precise way to study the MPT (by means of the morphology transition), and other aspects of mitochondrial dynamics, during cell death. In addition, our methodology allows a per-cell quantification of both chondriome morphology and cell death.

In both chemical and physical treatments, there was a tight correlation between the proportions of cells exhibiting abnormal mitochondria (probably as a result of the induction of a MPT) and those that went on to die 24–48 h later (Figs 4b,d, 5b,d); furthermore, 95% of dead cells had undergone a mitochondrial morphology transition (Fig. 5e). The changes in morphology observed during the study appeared to be mitochondria-specific, as there were no concomitant alterations in chloroplast shape or size after any of the treatments (see Supplementary Material Fig. S2).

The tight link between mitochondrial morphology and cell death is further strengthened by the results of experiments using the calcium channel-blocker LaCl₃ and the PTP inhibitor CsA. McCabe *et al.* (1997) demonstrated that inhibition of intracellular calcium flux could reduce cell death in plant cell cultures, while Yao *et al.* (2004) showed that CsA could partially inhibit protoporphyrin IX (PPIX)- and C2 ceramide-induced cell death. Our data suggest that these effects are associated with early changes in mitochondrial morphology, as use of LaCl₃ and CsA not only attenuates cell death, but also inhibits the mitochondrial morphology transition (Figs 6, 7). It is interesting to note that, while the two chemicals reduced cell death to similar extents, CsA showed a slightly smaller reduction in mitochondrial morphology change (Figs 6, 7). It is likely that this discrepancy is a manifestation of the fact that, while CsA prevents many mitochondria within a given protoplast from exhibiting a morphology transition (i.e. less than the 50% required in our assay), the threshold number of mitochondria that need to have undergone a transition to induce death is less than 50% of the total. Taken together, these data suggest that the mitochondrial morphology transition is not only an early indicator of subsequent cell death, but also a key mechanistic component of the cell death process.

The use of mild heat treatments to induce PCD has been reported in a variety of plant experimental systems and is proposed to induce a variety of biochemical responses, including the generation of intracellular ROS and the release of

cytochrome *c* (e.g. Balk *et al.*, 1999; Swidzinski *et al.*, 2002; Vacca *et al.*, 2004, 2006). However, the effect of a death-inducing mild heat shock on mitochondrial morphology remained unreported until now. Within 5 min of heat treatment, c. 70% of protoplasts displayed abnormal mitochondria indicative of a rapid morphology transition (Fig. 5b). While the heat-induced morphological transition was detected more rapidly than the changes elicited by chemical treatments (although not quantified, there was no obvious effect on mitochondrial morphology within 1 h of treatment with ROS), the nature and development of the mitochondrial morphology transition were otherwise very similar. This common response indicates that mitochondria are central to the cell death processes triggered by chemical or physical stress.

Strikingly, the alterations in mitochondrial morphology caused by heat or chemical treatments could be prevented by the addition of the synthetic, membrane-permeable, superoxide dismutase analogue TEMPOL (Figs 4c, 5c). These observations are consistent with those of Vacca *et al.* (2004), who showed that heat treatment of tobacco cell cultures produced a sharp rise in intracellular ROS, followed by loss of mitochondrial function and cell death. Adding purified superoxide dismutase to the cell culture medium reduced intracellular ROS and subsequent cell death (Vacca *et al.*, 2004). Our results suggest that both heat treatment and exogenously applied ROS-inducing chemicals increase *in vivo* ROS concentrations, which are sensed by the mitochondria. These changes lead to alterations in mitochondrial morphology at an early stage, and occur upstream of subsequent cell death.

While the cell death pathway in plants remains to be fully elucidated, a picture of the general steps can be inferred. Death stimuli, including biotoxins such as victorin (Curtis & Wolpert, 2004) and harpin (Krause & Durner, 2004), cell death protein substrate analogues (PPIX; Yao *et al.*, 2004); ROS (Yoshinaga *et al.*, 2005; this paper), senescence-induced PCD (Zottini *et al.*, 2006) and heat treatment (Balk *et al.*, 1999; Swidzinski *et al.*, 2002; Vacca *et al.*, 2004; Vacca *et al.*, 2006; this paper), are sensed either directly or indirectly by mitochondria. This leads to a change in mitochondrial morphology within several minutes, observed as matrix swelling during the onset of a change in mitochondrial permeability. This change in permeability induces a number of downstream effects eventually leading to the controlled destruction of the cell and its components: (1) within 1–4 h, there is a loss of $\Delta\Psi_m$ (Krause & Durner, 2004; Yao *et al.*, 2004); (2) there is release of cytochrome *c* at 2–4 h, either through rupture of the outer mitochondrial membrane (Balk *et al.*, 1999; Sun *et al.*, 1999; Arpagaus *et al.*, 2002) or by means of a membrane channel (Vacca *et al.*, 2004, 2006); (3) within 3–6 h, released cytochrome *c* may activate cytosolic caspase-like proteases which start to dismantle cellular components (Vacca *et al.*, 2006), resulting in eventual cell death, observable through biochemical measurements such as DNA laddering from 6 h onwards (McCabe & Leaver, 2000; Yao *et al.*, 2004, 2006).

What is clear from our results, however, is that the mitochondrion, and specifically modification of mitochondrial morphology, probably through perturbations in the permeability of the inner mitochondrial membrane, are a central feature of cell death in plants, as in other mitochondriate eukaryotes.

Acknowledgements

The work reported in this paper was carried out in the laboratory of Dr Alyson K. Tobin (University of St Andrews). We thank Mr Harry Hodge for technical assistance in the laboratory, growth rooms and glasshouse. This work was funded by Biotechnology and Biological Sciences Research Council research grants (DCL), and a studentship and Wain International Travel Fellowship to IS.

References

- Arpagaus S, Rawlyer A, Braendle R. 2002. Occurrence and characteristics of the mitochondrial permeability transition in plants. *Journal of Biological Chemistry* 277: 1780–1787.
- Balk J, Leaver CJ. 2001. The PET1-CMS mitochondrial mutation in sunflower is associated with premature programmed cell death and cytochrome *c* release. *Plant Cell* 13: 1803–1818.
- Balk J, Leaver CJ, McCabe PF. 1999. Translocation of cytochrome *c* from the mitochondria to the cytosol occurs during heat-induced programmed cell death in cucumber plants. *FEBS Letters* 463: 151–154.
- Curtis MJ, Wolpert TJ. 2002. The oat mitochondrial permeability transition and its implication in victorin binding and induced cell death. *Plant Journal* 29: 295–312.
- Curtis MJ, Wolpert TJ. 2004. The victorin-induced mitochondrial permeability transition precedes cell shrinkage and biochemical markers of cell death, and shrinkage occurs without loss of membrane integrity. *Plant Journal* 38: 244–259.
- Frank S, Gaume B, Bergmann-Leitner ES, Leitner WW, Robert EG, Catez F, Smith CL, Youle RJ. 2001. The role of dynamin-related protein 1, a mediator of mitochondrial fission, in apoptosis. *Developmental Cell* 1: 515–525.
- Frank S, Robert EG, Youle RJ. 2003. Scission, spores, and apoptosis: a proposal for the evolutionary origin of mitochondria in cell death induction. *Biochemical Biophysical Research Communications* 304: 481–486.
- Halliwell B, Gutteridge JM. 1985. *Free radicals in biology and medicine*. Oxford, UK: Clarendon Press.
- Ikeda Y, Ohki S, Koizumi K, Tanaka A, Watanabe H, Kohno H, van Rensen JJ, Boger P, Wakabayashi K. 2003. Binding site of novel 2-benzylamino-4-methyl-6-trifluoromethyl-1,3,5-triazine herbicides in the D1 protein of Photosystem II. *Photosynthesis Research* 77: 35–43.
- Jagasia R, Grote P, Westermann B, Conrath B. 2005. DRP-1-mediated mitochondrial fragmentation during EGL-1-induced cell death in *C. elegans*. *Nature* 433: 754–760.
- Krause M, Durrer J. 2004. Harpin inactivates mitochondria in Arabidopsis suspension cells. *Molecular Plant–Microbe Interactions* 17: 131–139.
- Laight DW, Andrews TJ, Haj-Yehia AI, Carrier MJ, Anggard EE. 1997. Microassay of superoxide anion scavenging activity in vitro. *Environmental Toxicology and Pharmacology* 3: 65–68.
- Lam E, Kato N, Lawton M. 2001. Programmed cell death, mitochondria and the plant hypersensitive response. *Nature* 411: 848–853.
- Latifi A, Jeanjean R, Lemeille S, Havaux M, Zhang C-C. 2005. Iron starvation leads to oxidative stress in *Anabaena* sp. strain PCC 7120. *Journal of Bacteriology* 187: 6596–6598.
- Lee WK, Thevenod F. 2006. A role for mitochondrial aquaporins in cellular life-and-death decisions? *American Journal of Cell Physiology* 291: C195–C202.
- Lee YJ, Jeong SY, Karbowski M, Smith CL, Youle RJ. 2004. Roles of the mammalian mitochondrial fission and fusion mediators Fis1, Drp1, and Opa1 in apoptosis. *Molecular Biology of the Cell* 15: 5001–5011.
- Liu X, Kim CN, Yang J, Jemmerson R, Wang X. 1996. Induction of apoptotic program in cell-free extracts: requirement for dATP and cytochrome *c*. *Cell* 86: 147–157.
- Logan DC. 2006. The mitochondrial compartment. *Journal of Experimental Botany* 57: 1225–1243.
- Logan DC, Leaver CJ. 2000. Mitochondria-targeted GFP highlights the heterogeneity of mitochondrial shape, size and movement within living plant cells. *Journal of Experimental Botany* 51: 865–871.
- Logan DC, Scott I, Tobin AK. 2003. The genetic control of plant mitochondrial morphology and dynamics. *Plant Journal* 36: 500–509.
- Logan DC, Scott I, Tobin AK. 2004. ADL2a, like ADL2b, is involved in the control of higher plant mitochondrial morphology. *Journal of Experimental Botany* 55: 783–785.
- McCabe PF, Leaver CJ. 2000. Programmed cell death in cell cultures. *Plant Molecular Biology* 44: 359–368.
- McCabe PF, Levine A, Meijer PJ, Tapon NA, Pennell RI. 1997. A programmed cell death pathway activated in carrot cells cultured at low cell density. *Plant Journal* 12: 267–280.
- Nunes-Nesi A, Fernie AR. 2007. Mitochondrial metabolism. In: Logan DC, ed. *Plant mitochondria*. Oxford, UK: Blackwell, 212–277.
- Okamoto K, Shaw JM. 2005. Mitochondrial morphology and dynamics in yeast and multicellular eukaryotes. *Annual Review of Genetics* 39: 503–536.
- Palmeira CM, Moreno AJ, Madeira VM. 1995. Mitochondrial bioenergetics is affected by the herbicide paraquat. *Biochimica et Biophysica Acta* 1229: 187–192.
- Scheffler IE. 1999. *Mitochondria*. New York, NY, USA: Wiley-Liss.
- Scott I. 2006. Control of mitochondrial morphology and dynamics in *Arabidopsis thaliana*. PhD thesis, University of St Andrews, St Andrews, UK.
- Scott I, Tobin AK, Logan DC. 2006. BIGYIN, an orthologue of human and yeast FIS1 genes functions in the control of mitochondrial size and number in *Arabidopsis thaliana*. *Journal of Experimental Botany* 57: 1275–1280.
- Skulachev VP. 1996. Why are mitochondria involved in apoptosis? Permeability transition pores and apoptosis as selective mechanisms to eliminate superoxide-producing mitochondria and cell. *FEBS Letters* 397: 7–10.
- Stickens D, Verbelen JP. 1996. Spatial structure of mitochondria and ER denotes changes in cell physiology of cultured tobacco protoplasts. *Plant Journal* 9: 85–92.
- Sun YL, Zhao Y, Hong X, Zhai ZH. 1999. Cytochrome *c* release and caspase activation during menadione-induced apoptosis in plants. *FEBS Letters* 462: 317–321.
- Swidzinski JA, Sweetlove LJ, Leaver CJ. 2002. A custom microarray analysis of gene expression during programmed cell death in *Arabidopsis thaliana*. *Plant Journal* 30: 431–446.
- Tsang EW, Bowler C, Herouart D, Van Camp W, Villarreal R, Genetello C, Van Montagu M, Inze D. 1991. Differential regulation of superoxide dismutases in plants exposed to environmental stress. *Plant Cell* 3: 783–792.
- Tsujimoto Y, Nakagawa T, Shimizu S. 2006. Mitochondrial membrane permeability transition and cell death. *Biochimica et Biophysica Acta* 1757: 1297–1300.
- Tzagoloff A. 1982. *Mitochondria*. New York, NY, USA: Plenum Press.
- Vacca RA, de Pinto MC, Valenti D, Passarella S, Marra E, De Gara L. 2004.

Production of reactive oxygen species, alteration of cytosolic ascorbate peroxidase, and impairment of mitochondrial metabolism are early events in heat shock-induced programmed cell death in tobacco Bright-Yellow 2 cells. *Plant Physiology* 134: 1100–1112.

Vacca RA, Valenti D, Bobba A, Merafina RS, Passarella S, Marra E.

2006. Cytochrome *c* is released in a reactive oxygen species-dependent manner and is degraded via caspase-like proteases in tobacco Bright-Yellow 2 cells en route to heat shock-induced cell death. *Plant Physiology* 141: 208–219.

Yao N, Eisfelder BJ, Marvin J, Greenberg JT. 2004. The mitochondrion – an organelle commonly involved in programmed cell death in *Arabidopsis thaliana*. *Plant Journal* 40: 596–610.

Yoshinaga K, Arimura SI, Niwa Y, Tsutsumi N, Uchimiya H, Kawai-Yamada M. 2005. Mitochondrial behaviour in the early stages of ROS stress leading to cell death in *Arabidopsis thaliana*. *Annals of Botany* 96: 337–342.

Youle RJ, Karbowski M. 2005. Mitochondrial fission in apoptosis. *Nature Reviews Molecular Cell Biology* 6: 657–663.

Yu T, Fox RJ, Burwell LS, Yoon Y. 2005. Regulation of mitochondrial fission and apoptosis by the mitochondrial outer membrane protein hFis1. *Journal of Cell Science* 118: 4141–4151.

Zoratti M, Szabo I. 1995. The mitochondrial permeability transition. *Biochimica et Biophysica Acta* 1241: 139–176.

Zoratti M, Szabo I, De Marchi U. 2005. Mitochondrial permeability transitions: how many doors to the house? *Biochimica et Biophysica Acta* 1706: 40–52.

Zottini M, Barizza E, Bastianelli F, Carimi F, Lo Schavo F. 2006. Growth and senescence of *Medicago truncatula* cultured cells are associated with characteristic mitochondrial morphology. *New Phytologist* 172: 239–247.

Zou H, Henzel WJ, Liu X, Lutschg A, Wang X. 1997. Apaf-1, a human protein homologous to *C. elegans* CED-4, participates in cytochrome *c*-dependent activation of caspase-3. *Cell* 90: 405–413.

Supplementary Material

The following supplementary material is available for this article online:

Fig. S1 Abnormal mitochondrial morphology in protoplasts following chemical or physical cell death-inducing treatments.

Fig. S2 Chloroplast morphology in protoplasts following chemical or physical cell death-inducing treatments.

This material is available as part of the online article from <http://www.blackwell-synergy.com/doi/abs/10.1111/j.1469-8137.2007.02255.x>

(This link will take you to the article abstract.)

Please note: Blackwell Publishing are not responsible for the content or functionality of any supplementary materials supplied by the authors. Any queries (other than about missing material) should be directed to the *New Phytologist* Central Office.



About *New Phytologist*

- *New Phytologist* is owned by a non-profit-making **charitable trust** dedicated to the promotion of plant science, facilitating projects from symposia to open access for our Tansley reviews. Complete information is available at www.newphytologist.org.
- Regular papers, Letters, Research reviews, Rapid reports and both Modelling/Theory and Methods papers are encouraged. We are committed to rapid processing, from online submission through to publication 'as-ready' via *OnlineEarly* – our average submission to decision time is just 28 days. Online-only colour is **free**, and essential print colour costs will be met if necessary. We also provide 25 offprints as well as a PDF for each article.
- For online summaries and ToC alerts, go to the website and click on 'Journal online'. You can take out a **personal subscription** to the journal for a fraction of the institutional price. Rates start at £135 in Europe/\$251 in the USA & Canada for the online edition (click on 'Subscribe' at the website).
- If you have any questions, do get in touch with Central Office (newphytol@lancaster.ac.uk; tel +44 1524 594691) or, for a local contact in North America, the US Office (newphytol@ornl.gov; tel +1 865 576 5261).